PAPER • OPEN ACCESS

Markovian heat sources with the smallest heat capacity

To cite this article: Raam Uzdin *et al* 2018 *New J. Phys.* **20** 063030

New Journal of Physics
The open access journal at the forefront of physics

Deutsche Physikalische Gesellschaft DPG
IOP Institute of Physics

Published in partnership with: Deutsche Physikalische Gesellschaft and the Institute of Physics

OPEN ACCESS

RECEIVED
27 March 2018

REVISED
24 May 2018

ACCEPTED FOR PUBLICATION
31 May 2018

PUBLISHED
20 June 2018

PAPER

Markovian heat sources with the smallest heat capacity

Raam Uzdin[1,2], **Simone Gasparinetti**[3], **Roee Ozeri**[4] **and Ronnie Kosloff**[2]

[1] Technion-Isreal Institute of Technology, Haifa, 3200008, Israel
[2] Hebrew University of Jerusalem, Jerusalem 9190401, Israel
[3] Department of Physics, ETH Zurich, CH-8093 Zurich, Switzerland
[4] Department of Physics of Complex Systems, Weizmann Institute of Science, Rehovot, 7610001, Israel

E-mail: raam@mail.huji.ac.il

Keywords: open quantum systems, quantum thermodynamics, Zeno, small heat sources, non-Markovian corrections

Abstract

Thermal Markovian dynamics is typically obtained by coupling a system to a sufficiently hot bath with a large heat capacity. Here we present a scheme for inducing Markovian dynamics using an arbitrarily small and cold heat bath. The scheme is based on injecting phase noise to the small bath. Markovianity emerges when the dephasing rate is larger than the system-bath coupling. Several unique signatures of small baths are studied. We discuss realizations in ion traps and superconducting qubits and show that it is possible to create an ideal setting where the system dynamics is indifferent to the internal bath dynamics.

Thermodynamics of small systems have been intensively studied in recent years. Stochastic thermodynamics explores the relations between different trajectories in the system phase space [1, 2]. Quantum thermodynamics [3–5] deals with the effects of non-classical dynamics and non-classical features such as coherence and entanglement on thermodynamics. Apart from the practical importance of understanding and experimenting with thermodynamics at the smallest scales, the study of quantum thermodynamics has also provided exciting theoretical developments. As an example, it has been shown that there are additional second law-like constraints on small systems interacting with a thermal bath [6–8]. In addition, there are thermodynamic effects in heat machines that can be observed only in systems that are sufficiently 'quantum' [9–12]. Furthermore, some quantum heat machine setups can exceed classical/stochastic bounds [10, 11].

In a self-contained nanoscale setup (e.g. ion traps) that includes the baths, the heat capacities of the baths will be nanoscopic as well. How small can an object be and still perform as a thermal bath? What are the features of a large bath that a microscopic heat bath ('microbath') can mimic? The most pronounced feature of a large ideal bath is its lack of memory. Given the state of the system and the bath temperature, the change in the state of the system is fully determined. Moreover, the asymptotic state of the system will be a thermal state with the original bath temperature. To achieve this, the bath has to have a short correlation time with respect to the system-bath coupling strength [13]. For this the bath has to be very large and often also sufficiently hot. In collision type baths [14–21] the bath can be very cold since the short correlation time is achieved by many weak and fast collisions with the system. The bath is assumed to be large so that each bath particle collides with the system only once. In this paper, we suggest a scheme for a bath that generates Markovian dynamics for (1) arbitrary low temperature, and (2) arbitrary small heat capacity (see appendix A for heat capacity of small baths).

Interaction with a small environment will typically involve large oscillations and non-Markovian effects. To obtain the desired result (e.g. thermalization), the interaction with the bath has to be switched off at a specific time. Although these oscillations can be exploited [9], it is often desirable to have protocols where the system relaxes monotonically (and quickly) to the desired state. In Markovian dynamics, it is sufficient to wait a few relaxation times to ensure the system is prepared in the desired state, and there is no need to stop the dynamics at a specific point in time.

Our microbath consists of a small ensemble of two-level systems (spins) coupled to each other and to the system by either local interactions (nearest neighbor (NN) in a one-dimensional chain), or global interactions ('all to all' (ATA) in this paper). The microbath spins are subjected to externally induced, uncorrelated

dephasing. In the limit in which the dephasing rate is much larger than the coupling rate, we show that the microbath induces a Markovian dynamics on the system. This result is exact for global interactions, while for local interactions it requires the additional assumption of weak system-bath coupling. The smallness of the microbath manifests itself in two distinct features: a dependence of the equilibration state on the initial state of the system, and an enhancement of the dephasing time with respect to the population decay time.

General setup

The heat source (microbath) is an ensemble of N spins. Excluding the external dephasing source, the Hamiltonian that describes our setup is

$$H_{\rm tot} = H_0 + V = h_0 \sum_{i}^{N+1} \sigma_i^z + \sum_{i>j}^{N+1} V_{ij}, \tag{1}$$

where σ_i^z is the Pauli z matrix of spin i. The first N spins constitute the microbath, and spin $N+1$ is the system. Alternatively, the system can be larger but the bath interacts only with two levels in the system as often the case in quantum heat machines [10, 22, 23]. The spin–spin energy conserving interactions (between the system and the bath or between the bath spins) are of the form

$$V_{ij} = \xi_{ij}(\sigma_i^- \sigma_j^+ + \sigma_i^+ \sigma_j^-), \tag{2}$$

where $\sigma_i^{+(-)}$ is the creation (annihilation) operator of spin i. The first configuration we study is ATA coupling, where all spins are equally coupled to each other $\xi_{ij} = \xi$. The second configuration is a linear chain with NN coupling $\xi_{ij} = \xi_{ij}\delta_{i,j+1}$. While the NN is the most simple and natural bath model, we find that the ATA has a useful thermodynamic property that distinguishes it from other configurations. These two configurations can be implemented in ion traps and superconducting circuits as discussed at the end of the paper. See [24] for experimental realization with one hundred spins.

When N is a small number and there is no dephasing, frequent quantum recurrences takes place and energy oscillates back and forth between the system and the microbath. In general, the system will not relax to a steady state.

Dephased baths—adding an extra dephasing environment

In our setup, each *microbath* spin (1 to N) is subjected to dephasing (phase damping) created by some larger environment. Strong dephasing can be an intrinsic, possibly tunable, property of the spin system [25], or it can be artificially induced by noise engineering (see experimental setup below). The spin decoherence dynamics is described by a Lindblad equation as described in appendix B. The coherence relaxation rate is denoted by α. Alternatively, the dephasing can be replaced by repeated projective energy measurements (σ^z) of the spins in the bath. The typical time between subsequent measurements will determine the effective dephasing rate α. In appendix C it is explained why the dephasing environment is a free resource. In our scheme, the microbath is dephased but the system is not dephased. Hence, it is quite different from other proposals [26–30].

In addition to coherence between energy eigenstates of each spin in the bath, dephasing also eliminates coherence between multiparticle states (e.g. $|01\rangle + e^{i\phi}|10\rangle$). We show that when this inter-particle coherence mitigation is larger than the coupling rates, recurrences are eliminated and Markovian dynamics is observed. Let z_s denote the polarization of the system spin $z_s = {\rm tr}[\sigma_{N+1}^z \rho]$. In appendix B we show that for the ATA and NN configurations (NN also requires weak system-bath coupling), strong dephasing leads to the following equation of motion

$$\frac{{\rm d}^2}{{\rm d}t^2} z_s = 2\xi_{\rm SB}^2 \frac{N+1}{N}(z_\infty - z_s) - \alpha \frac{\rm d}{{\rm d}t} z_s, \tag{3}$$

$$z_\infty = \frac{\sum_{i=1}^{N+1} z_i(0)}{N+1} = \frac{N}{N+1} z_T + \frac{1}{N+1} z_s(0), \tag{4}$$

where z_T is the initial average polarization of the microbath spins, and is equal to $z_T = -\tanh[h_0/(2T)]$ given that the microbath is prepared in a thermal state of temperature T. In deriving (3), we have neglected terms of order $\frac{\xi_{\rm SB}^2}{\alpha^2}$ (see appendix B). For the ATA case $\xi_{\rm SB}^2 = N\xi^2$, and for the NN configuration $\xi_{\rm SB}^2 = \xi_{N,N+1}^2$. z_∞ is the polarization of the system after it fully equilibrates with the microbath to a state where all the $N+1$ spins have the same polarization. The dependence of z_∞ on the system initial state is a direct consequence of having a heat source with initial energy that is not overwhelmingly larger than that of the system (i.e., small heat capacity, see also [31]).

For the system coherence, for example $x_s = \mathrm{tr}[\sigma^x_{N+1}\rho]$, the situation is somewhat simpler since the bath has no initial coherence and we obtain

$$\frac{\mathrm{d}^2}{\mathrm{d}t^2}x_s = \xi_{\mathrm{SB}}^2 x_s - \alpha\frac{\mathrm{d}}{\mathrm{d}t}x_s. \tag{5}$$

General features of the reduced dynamics

We start by studying the different regimes of operation depending on the value of α/ξ_{SB}. Equation (3) reveals that the only solution consistent with strong dephasing $\alpha/\xi_{\mathrm{SB}} \to \infty$ is the Zeno freeze-out $\frac{\mathrm{d}}{\mathrm{d}t}z_s(t) = 0$. This feature can be useful to decouple the system from the bath without changing ξ_{SB}. The next regime of interest is that of Markovian dynamics. As α gets smaller and closer in magnitude to ξ_{SB}, the system starts to evolve in a Markovian manner. By neglecting the second derivative in (3) we get a Markovian equation, and its solution is

$$z_s^{\mathrm{Mark}} = z_\infty + (z_s(0) - z_\infty)\exp\left[-\frac{2\xi_{\mathrm{SB}}^2}{\alpha}\frac{N+1}{N}t\right]. \tag{6}$$

In accordance with the Zeno freeze-out, the thermalization rate satisfies $\frac{\xi_{\mathrm{SB}}^2}{\alpha}\frac{N+1}{N} \to 0$ when $\alpha \ggg \xi_{\mathrm{SB}}$. By evaluating $\frac{\mathrm{d}^2}{\mathrm{d}t^2}z_s^{\mathrm{Mark}}$, and dividing by ξ_{SB}^2 we find that it is $O\left[\left(\frac{\xi_{\mathrm{SB}}}{\alpha}\right)^2\right]$ whereas the other terms are $O\left[\left(\frac{\xi_{\mathrm{SB}}}{\alpha}\right)^0\right]$. Thus, Markovian dynamics is observed when the dephasing is sufficiently larger than the system-bath coupling strength ($\alpha \gg \xi_{\mathrm{SB}}$). In practice, when the dephasing rate is roughly an order of magnitude larger than the coupling coefficient, the dynamics is already highly Markovian.

For a microbath initially prepared at temperature T, a system in a thermal state with temperature T is a *fixed point* of the setup. The *asymptotic state* is the state that a non-thermal state will reach after a very long time with respect to the thermalization time. In large baths, the asymptotic state and the fixed point are the same. The situation is different in small baths. While the thermal state is still a fixed point of thermalization maps, the asymptotic state is given by z_∞, and not by the polarization of a thermal state z_T determined by the initial temperature of the bath. From the definition of z_∞ one can verify that in the large bath limit $N \gg 1$, $z_\infty \to z_T$ and the asymptotic state becomes equal to the fixed point. As shown in appendix A, the heat capacity is proportional to the number of spins in the bath $C_v = N\left(\frac{h_0}{2T}\right)^2 \mathrm{sech}^2\frac{h_0}{2T}$. Thus, when the heat capacity is very large with respect to $\left(\frac{h_0}{2T}\right)^2 \mathrm{sech}^2\frac{h_0}{2T}$, then $z_\infty \to z_T$ and the fixed point and the asymptotic state become the same. Asymptotic states are of great interest in the context of dissipative quantum state engineering [32] and entanglement creation by heat machines [33, 34].

The large α/ξ_{SB} limit of (5) leads to Markovian dynamics for the coherence $x_s^{\mathrm{Mark}} = x_s(0)\exp[-\frac{\xi_{\mathrm{SB}}^2}{\alpha}t]$. Comparing the exponential decay rate of the coherence and polarization we find $\gamma_z = 2\frac{N+1}{N}\gamma_x$ where $\gamma_x = \frac{\xi_{\mathrm{SB}}^2}{\alpha}$ (see equation (5)). As shown in appendix D, the $\frac{N+1}{N}$ enhancement of the decay rate with respect to twice the dephasing rate, *is an effect unique to small heat capacity baths*. This enhancement is not in contradiction to the known $\gamma_z \leqslant 2\gamma_x$ ($T_2 \leqslant 2T_1$) relation, valid for completely positive *time-independent* Markovian maps [35, 36]. The $\frac{N+1}{N}$ enhancement, is due to non-negligible changes in the average populations of the bath (for $N = O(1)$). See appendix D for further details. This enhanced decay rate is an experimentally measurable signature of small dephased baths. A large Markovian bath with the same population decay time $T_1 = \gamma_z$ cannot generate decoherence time $T_2 = 1/\gamma_x$ as high as $2\frac{N+1}{N}T_1$.

Closed form non-Markovian reduced dynamics

Starting at $t = 0$ without system-bath coherence implies $\frac{\mathrm{d}}{\mathrm{d}t}z(0) = 0$. Thus, at early times before the system starts to follow Markovian dynamics [13, 37], the second derivative in (3) dominates. This second derivative is a reminiscent of the unitary dynamics that takes place in the absence of dephasing. Unlike more complicated setups with strong memory effects, here all the non-Markovian effects are encapsulated in the second derivative term. A numerical example is given below.

ATA configuration

In this configuration $\xi_{\mathrm{SB}}^2 = N\xi^2$. The N factor in ξ_{SB}^2 is expected since the system is connected to N spins. In the numerical example in figure 1 we use a three-spin microbath that interacts with a system (another spin) via ATA coupling. The parameters are $\xi = 1$ and $\alpha = 6$. The dashed-black curve in figure 1(a) shows the Markovian approximation (6) with respect to the exact dynamics (red curve). A most appealing feature of the ATA configuration is that the reduced dynamics of the system does not depend on the internal polarization variation

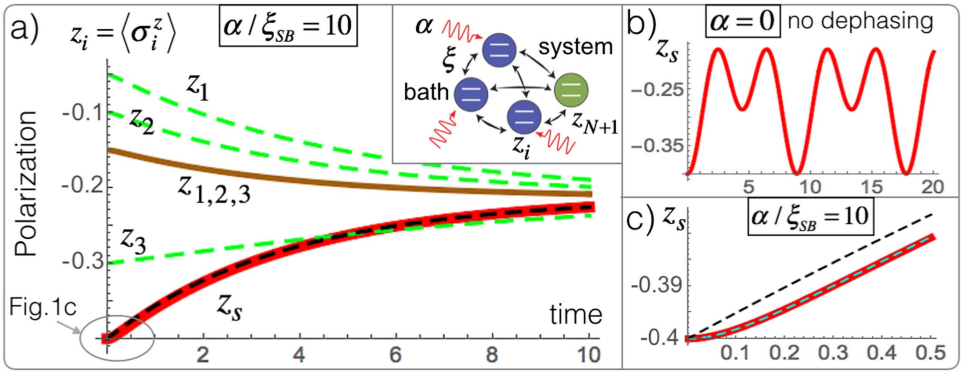

Figure 1. (a) System polarization (z_s) and bath spin polarization ($z_i, i = 1, 2, 3$) versus time in the all to all configuration (inset) with bath dephasing rate of $\alpha = 10\xi_{\rm SB}$. Remarkably, in this configuration the system dynamics is the same whether the bath is initially prepared in a uniform thermal state (brown), or in any other state with the same total initial polarization (green). Thus, this scheme performs as an ideal small heat source. The Markovian approximation (dashed-black) accurately describes the exact system dynamics (red). (b) Without external dephasing ($\alpha = 0$) the system does not equilibrate at all. (c) Although the Markovian approximation fails at very short times, the dynamics is still accurately described by (3) (cyan).

in the bath. Only the total polarization of the bath (total energy) affects the system (see SM for more information). This means that to get a thermalization dynamics there is no need to carefully prepare the bath in a (global) thermal state. This feature is a major simplification both from the practical (or experimental) point of view and from the theoretical point of view. The green-dashed curves in figure 1(a) shows that a completely different bath preparation with the same initial total polarization, leads to the exact same system dynamics (analytically the same, so no deviations in the system dynamics can be seen in the graph). Moreover, even strong classical correlation in the bath (e.g. $(1-p)|000\rangle\langle 000| + p|111\rangle\langle 111|$) will not affect the reduced dynamics of the system. In figure 1(b), free evolution without external dephasing is plotted. Quantum recurrences dominate the dynamics and equilibrium is not achieved.

Figure 1(c) shows that (3) accurately describes the short-time non-Markovian evolution. For short-time-evolution the second derivative in (3) is highly important even if $\alpha \gg \xi_{\rm SB}$.

In large baths without dephasing, weak system-bath coupling is crucial for observing Markovian dynamics. The coupling has to be smaller than the bath correlation time, which depends on the bath temperature [13] . As a result, the Lindblad description fails for very cold baths (excluding collision baths which can be cold, but cannot be small and Markovian as well). In contrast, *in our setup there is no such limitation*. The system-bath coupling has to be small compared to the dephasing rate. Under sufficiently strong dephasing the system will follow Markovian dynamics *regardless of how cold* is the initial temperature of the bath and how small the microbath is. The fact that the dephased bath can be highly out of equilibrium can be considered as strong system-environment coupling effect (in the ATA configuration). Yet, this is very different from other strong coupling studies where the interaction dresses the system but the bath is still large [38–41].

Weak versus strong coupling in dephased baths

When the coupling of the system to the bath $\xi_{\rm SB}$ is much weaker than the coupling between different spins in the microbath ξ_{ij}^B $(i, j < N+1)$ the dynamics greatly simplifies. In the presence of dephasing and $\xi_{ij}^B \gg \xi_{\rm SB}$, the microbath spins equilibrate among themselves before the system changes significantly. Thus, (3) is valid also for configurations such as NN with weak system-bath coupling (see appendix B). In appendix B we write an equation similar to (3) for the NN configuration when $\xi_{ij}^B \gg \xi_{\rm SB}$ does not hold.

System-bath correlation in small dephased baths

Next, we study the creation of system-bath correlation during Markovian and non-Markovian dynamics of the system. When the system is weakly coupled to a *large* bath, the correlation between the system and the bath can be made negligible and be ignored. This is not the case for small baths. In the following, we discuss both the NN and the ATA configurations. As an illustrative example in the NN setup we use a three-spins microbath with $\alpha = 6, \xi_B = 1$ and $\xi_{\rm SB} = 1/20$. For the ATA setup we use the same setup but with $\alpha = 6$, $\xi = 1/(20\sqrt{3})$. As a result, the Markovian decay time for both configurations is the same, and is equal to $\tau_{\rm MARK} = \alpha/(2\xi_{\rm SB}^2) = 1200$. The top curves in figure 2(a) show that the system polarization in the NN configuration (red curve), and the polarizations in the ATA configuration (dashed-blue) have practically the same evolution. The tiny differences (not visible in the figure) arise from the fact that the microbath spins (lower curves show z_1, z_2, z_3) do not yet perfectly equilibrate among themselves. Corrections to Markovian dynamics are observed only on a timescale of

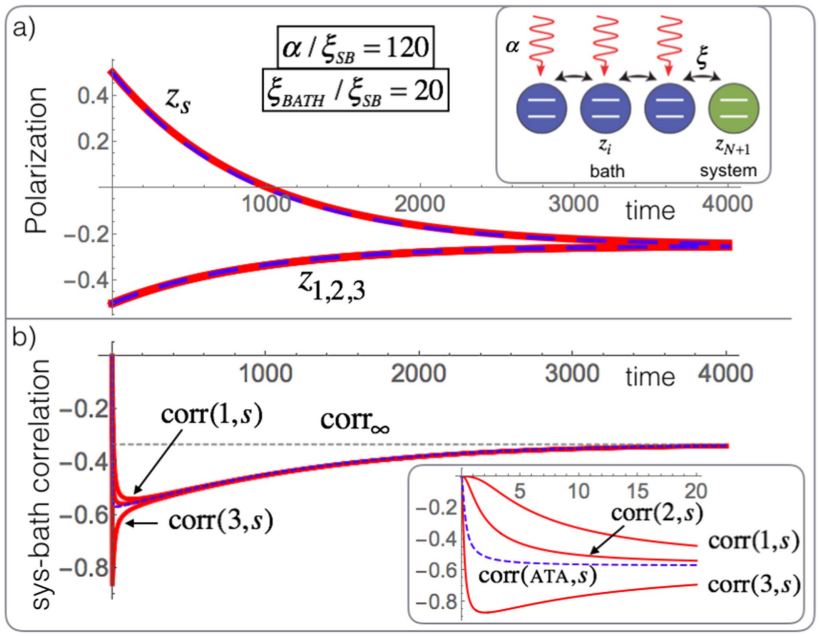

Figure 2. Strong system-bath correlation can form even when the system follows Markovian dynamics. (a) In the weak coupling limit in the NN configuration (see inset), the polarization dynamics (red curves) is the same as that of the ATA configuration (blue dashed curves) when the ATA configuration is set to have the same decay time $\alpha/(2\xi_{SB})^2$. Yet, the system-bath correlation (b) in the NN setup (red) is non-uniform even when the bath polarization is highly uniform (see inset). The ATA correlation is shown in the dashed-blue curve. While the peak correlation depends on the setup parameters, the unavoidable asymptotic correlation corr_∞ (7) is fixed by the initial conditions and cannot be mitigated by weak system-bath coupling.

$1/\alpha = 1/6$. We study correlations using the standard statistical correlation function $\mathrm{corr}(i,j) = \mathrm{cov}(z_i, z_j)/[\mathrm{var}(z_i)\mathrm{var}(z_i)]$. The dashed-blue curve in figure 2(b) shows the correlation between any of the bath spins and the system in the ATA configuration. A more interesting dynamics takes place in the NN setup. These correlations are classical since off diagonal elements are negligible in the presence of strong dephasing. Remarkably, even though the bath spins in the NN case have almost exactly the same polarizations (figure 2(a)), their correlations with the system differ significantly at $1/\alpha \leqslant t \ll \tau_{\mathrm{MARK}}$ as shown by the red curves in figure 2(b) (see the inset for a magnification). This highly interesting correlation equilibration at a rate much slower than the polarization equilibration warrants further study.

Another interesting feature in the correlation evolution is the asymptotic value obtained for $t \gg \tau_{\mathrm{MARK}}$. While the transient correlation evolution depends on the coupling strength and on the coupling configuration, the asymptotic value corr_∞ depends only on the initial conditions. This can be understood from the fact that $\sum_{i\neq j}^{N+1}\langle\sigma_i^z\sigma_j^z\rangle$ is a conserved quantity for any choice of ξ_{ij}. Using this conserved quantity together with energy conservation, and the fact that the final equilibrium state is completely uniform, we obtain the asymptotic correlation $\mathrm{corr}_\infty = \left[\frac{1}{(N-1)N}\sum_{i\neq j}^{N+1}\langle\sigma_i^z\sigma_j^z\rangle_{t=0} - z_\infty^2\right]/(1/4 - z_\infty^2)$. When the spins are initially uncorrelated and the bath starts in a uniform polarization this expression simplifies to

$$\mathrm{corr}_\infty = -\frac{(z_T - z_s(0))^2}{(M+1)^2}/(1/4 - z_\infty^2). \tag{7}$$

Note that regardless of the configuration, at $t \to \infty$ the system is equally correlated to *all* bath spins. corr_∞ is negative for any M, z_T, and $z_s(0)$. Moreover, since $z_\infty \to z_T$ for large N, we conclude from (7) that the asymptotic correlation scales like $1/(M+1)^2$ when z_T and $z_s(0)$ are kept fixed. Hence, $\mathrm{corr}_\infty \to 0$ for large bath. Thus, the unavoidable asymptotic system-bath correlation is another unique feature that appears in small dephased baths, even when the dynamics is fully Markovian. In small *non-dephased* baths the correlation will also be strong but the correlation will oscillate without reaching a steady state.

Experimental realization in ion traps

Quantum simulation of spin Hamiltonians has been demonstrated using trapped atomic ions [42–44]. An effective spin 1/2 system (pseudo-spin) is realized using two internal levels of the ion which can be separated by radio-frequency, microwave, or optical transitions. By using spin-dependent forces that couple internal and translational degrees of freedom, it is possible to generate various interactions between the ions. In appendix E

we discuss NN and ATA realization in ion traps and find that it should be possible to implement a dephased bath scheme with the current experimental capabilities.

Experimental realization superconducting circuits

Dephased baths can also be readily implemented in superconducting circuits. By coupling transmon-type superconducting qubits [45] to a common far detuned resonator, the NN and the ATA configurations can be implemented. In appendix F we provide estimates and mention previously implemented building blocks. The superconducting architecture also allows to experimentally explore possible extensions of this work, including studies of system-bath correlations, continuously driven open system [46], etc.

Conclusions

We have introduced a paradigm for the implementation of Markovian heat sources with the smallest possible heat capacity. In contrast to oscillatory non-Markovian dynamics that typically arises when interacting with a small environment, Markovian dynamics have the advantage of monotonically converging to the desired asymptotic state. Thus there is no need to stop the dynamics at particular times to obtain the desired result. Despite the Markovian dynamics we have identified features in our setup that are unique to small heat sources: (1) an enhanced decay rate with respect to the decoherence rate (2) a significant, and unavoidable system-bath correlation that cannot be eliminated by reducing the system-bath coupling. In addition, we find a correlation equilibration time that is much larger than the bath polarization equilibration time. Finally, our theoretical approach also provides an accurate reduced description of the non-Markovian dynamics at short evolution times.

We have studied realizations in ion traps and in superconducting qubits where the ATA coupling can be implemented. In our dephased bath setup the ATA coupling has the remarkable property that the system is sensitive only to the *total* energy in the bath. This makes the ATA microbath an ideal microbath: the internal dynamics inside the microbath does not affect the reduced dynamics of the system. This greatly simplifies the preparation stage of the microbath: any preparation with the same energy will do.

Potentially, these microbaths can serve as a practical element in experiments. Furthermore, this setup motivates new questions about open quantum systems. For example, the study of accumulated system-bath correlation is a complicated topic that is greatly simplified in the dephased bath setup proposed here. In addition, it is intriguing to study dephasing in quantum systems with larger Hilbert space (qudits) and to include system-bath particle exchange.

Acknowledgments

This work was supported by the Israeli science foundation. The work of RO is supported by grants from the ISF, I-Core, ERC, Minerva and the Crown photonics center. SG and RU are grateful to J Heinsoo and Y Salathé for useful discussions.

Appendix A. Heat capacity of small baths

The heat capacity of a bath is defined as

$$C = \frac{Q}{\delta T}, \tag{8}$$

where Q is the heat exchanged with the bath upon a change of δT in the temperature of the bath. C is a measure of the bath size. This definition assumes that after taking Q amount of heat the bath returns to a thermal state that commensurate to the new energy of the bath. However, in small baths (even in the dephased ones considered in this paper) the final state is typically not a thermal state or even close to it. Nonetheless, the definition in (8) can still be useful. To define the heat capacity of a small bath we consider two additional *macroscopic* baths at temperatures T and $T' = T + \delta T$. We first thermalize the small bath by connecting it to the large bath at temperature T. This is repeated for bath T'. The heat flow Q (which is equal to the change in the energy of the small bath) is recorded and the small bath heat capacity is given by (8). Note that this process is an isochore (constant volume) since we did not change the energy levels of the small bath (no work involved, only heat). From this we get

$$C_v = \frac{Q}{T' - T}. \tag{9}$$

For a system of N non-interacting spins with energy gap h_0 the heat capacity (for very small δT) is

$$C_v = \frac{\mathrm{d}\langle E\rangle}{\mathrm{d}T} = N\left(\frac{h_0}{2T}\right)^2 \mathrm{sech}^2\frac{h_0}{2T}. \tag{10}$$

See [47] for a generic bound on the heat capacity of finite-dimension microbaths (Corollary 10 of theorem 8). Since $\left(\frac{h_0}{2T}\right)^2 \mathrm{sech}^2\frac{h_0}{2T} \leqslant 1/2$ the heat capacity of N non-interacting spins is smaller than $N/2$. Similarly, the heat capacity of the *system* can be defined as well. The standard Markovian limit for large bath requires that $C^{\mathrm{sys}} \ll C^{\mathrm{bath}}$.

The reason for considering the heat capacity of non-interacting spins is that in the presence of dephasing the stationary thermal state is not the one given by the full Hamiltonian with the interactions, but the thermal state of the bare spins.

Appendix B. Derivation of the equation of motion

The system-bath setup dynamics is modeled by a Lindblad equation

$$d_t\rho = -\mathrm{i}[H,\,\rho] + \sum_{k=1}^{N} 2A_k\rho A_k^\dagger - A_k^\dagger A_k\rho - \rho A_k^\dagger A_k, \tag{11}$$

where A_k describes the external dephasing environment, and H is given by equation (1) in the main text. By moving to the interaction picture H_0 is eliminated while V and A_k remains unaffected since they commute with H_0. To obtain a dephasing rate α for spin i we set $A_k = \sqrt{\alpha}\,\sigma_i^z$. Note that for two spins A_1 (or A_2) will also lead to dephasing at a rate α of coherences that involve both spins for example element $\rho_{2,3}$ in the joint density matrix.

We start the derivation of the equation of motion by writing the equation for the time derivative of polarization of the system spin $z_s = \langle\sigma_s^z\rangle$

$$d_t z_s = \mathrm{tr}\{-\mathrm{i}\sigma_s^z[V,\,\rho] + \sigma_s^z\sum_{k=1}^{N} 2A_k\rho A_k^\dagger - A_k^\dagger A_k\rho - \rho A_k^\dagger A_k\}. \tag{12}$$

Since $[A_k,\,\sigma^z] = 0$

$$d_t z_s = \mathrm{tr}[-\mathrm{i}\sigma_s^z(V\rho - \rho V)] = -\mathrm{itr}([\sigma_s^z,\,V]\rho).$$

In contrast to other methods for obtaining reduced dynamics that are based on integration (see the microscopic derivation [13]), we start with differentiation

$$\begin{aligned} d_t^2 z_s &= \mathrm{tr}\{-\mathrm{i}\sigma_s^z[H,\,d_t\rho] \\ &\quad + \sigma_s^z\sum_{k=1}^{N} 2A_k d_t\rho A_k^\dagger - A_k^\dagger A_k d_t\rho - d_t\rho A_k^\dagger A_k\} \qquad (13)\\ &= \mathrm{tr}\{-\sigma_s^z[V,\,[V,\,\rho]]\} \\ &\quad - \alpha\mathrm{tr}\left\{\mathrm{i}\sigma_s^z[V,\,\left(\sum_{k=1}^{N} 2\sigma_k^z\rho\sigma_k^z - \frac{1}{2}\rho\right)\right\}. \qquad (14)\end{aligned}$$

Let us first study the first term (quadratic in V)

$$\begin{aligned} \mathrm{tr}\{\sigma_s^z[V,\,[V,\,\rho]]\} &= \mathrm{tr}\{\rho[[\sigma_s^z,\,V],\,V]\} \\ &= \mathrm{tr}\{\rho[[\sigma_s^z,\,\sum_{k=1}^{N} V_{s,k}],\,\sum_{j=1}^{N+1} V_{k,j}]\} \\ &= \sum_{k}^{N}\mathrm{tr}\{\rho[[\sigma_s^z,\,V_{s,k}],\,V_{k,s}]\} \\ &\quad + \mathrm{tr}\{\rho[[\sigma_s^z,\,\sum_{k=1}^{N} V_{s,k}],\,\sum_{j=1}^{N} V_{k,j}]\} \\ &= \sum_{k=1}^{N} 2(z_s - z_k)\xi_{sk}^2 \\ &\quad + 2\sum_{k,j=1}^{N}\xi_{sk}\xi_{kj}\langle A\rangle, \end{aligned} \tag{15}$$

where

$$A = \sigma_j^- \sigma_k^z \sigma_s^+ + \text{h.c.}$$

We will show later on that the contribution form the A term is negligible. Next we study the second term in (14) (Linear in α)

$$\begin{aligned}\alpha \text{tr}\left\{ \text{i}\sigma_s^z [V, \left(\sum_{k=1}^{N} 2\sigma_k^z \rho \sigma_k^z - \frac{1}{2}\rho\right)\right\} &= \alpha \text{itr} \sum_{k=1}^{N} \rho \sigma_k^z [\sigma_s^z, V] \sigma_k^z \\ &= -\text{i}\alpha \text{tr} \sum_{k=1}^{N} \rho [\sigma_s^z, V] \\ &= \alpha d_t \langle z \rangle, \end{aligned} \tag{16}$$

where we have used the relation $\sigma^z \sigma^{\pm} \sigma^z = -\frac{1}{4}\sigma^{\pm}$. Finally, we get

$$\frac{\text{d}^2}{\text{d}t^2} z_s = -2 \sum_{k=1}^{N} \xi_{sk}^2 (z_s - z_k) - \alpha \frac{\text{d}z_s}{\text{d}t} + O(\xi^2 \langle A \rangle). \tag{17}$$

Next we wish to evaluate the magnitude of $\langle A \rangle$. Since A is a coherence (off diagonal element of the density matrix) the equation of motion of $\langle A \rangle$ is

$$\frac{\text{d}}{\text{d}t} \langle A \rangle = \langle -\text{i}[V, \rho] A \rangle - \alpha \langle A \rangle. \tag{18}$$

Using the fact that for $\alpha \gg \xi$ the dephasing dominates and the system quickly relaxes to inhomogeneous solution

$$\langle A \rangle = \frac{-\text{i}}{\alpha} \langle [V, \rho] A \rangle = \frac{-\text{i}}{\alpha} \langle [A, V] \rho \rangle. \tag{19}$$

After some algebra we get

$$[A, V] = \sigma_k^- \sigma_s^+ - \sigma_j^- \sigma_k^+ - \text{h.c.}$$

and therefore

$$\langle A \rangle \propto \frac{\xi}{\alpha} \langle \sigma_k^- \sigma_s^+ - \sigma_j^- \sigma_k^+ - \text{h.c.} \rangle. \tag{20}$$

However $\langle \sigma_k^- \sigma_s^+ - \sigma_j^- \sigma_k^+ - \text{h.c.} \rangle$ is a sum of coherences and therefore from (19)

$$\begin{aligned}\langle \sigma_k^- \sigma_s^+ - \sigma_j^- \sigma_k^+ - \text{h.c.} \rangle &= \frac{-\text{i}}{\alpha} \langle [\sigma_k^- \sigma_s^+ - \sigma_j^- \sigma_k^+ - \text{h.c.}, V] \rho \rangle \\ &= O(\xi/\alpha). \end{aligned} \tag{21}$$

Hence, from (20) and (21) we conclude that $\langle A \rangle = O(\xi^2/\alpha^2)$. Comparing $\xi^2 \langle A \rangle$ to the first term in the right hand side of (17) we find that it is ξ^2/α^2 smaller. Thus, this term can be safely neglected when $\alpha \gg \xi$ and we obtain

$$\frac{\text{d}^2}{\text{d}t^2} z_s = -2 \sum_{k=1}^{N} \xi_{sk}^2 (z_s - z_k) - \alpha \frac{\text{d}z_s}{\text{d}t}. \tag{22}$$

Note that in general $z_k = z_k(t)$ so this equation is not closed and cannot be solved without prior knowledge of $z_k(t)$. There are scenarios, though, in which this equation is closed, and can be solved. One is the ATA coupling, and the other is weak coupling. In the ATA coupling $\xi_{sk} = \xi$ so we can write

$$\begin{aligned}\frac{\text{d}^2}{\text{d}t^2} z_s &= -2\xi^2 N z_s + 2\xi^2 \sum_{k=1}^{N} (z_k) - \alpha \frac{\text{d}z_s}{\text{d}t} \\ &= -2\xi^2 N z_s + 2\xi^2 (z_{\text{tot}} - z_s) - \alpha \frac{\text{d}z_s}{\text{d}t} \\ &= -2\xi^2 (N+1) z_s - 2\xi^2 z_{\text{tot}} - \alpha \frac{\text{d}z_s}{\text{d}t} \\ &= -2\xi^2 (N+1) \left(z_s - \frac{z_{\text{tot}}}{N+1} \right) - \alpha \frac{\text{d}z_s}{\text{d}t}. \end{aligned} \tag{23}$$

Finally, we get

$$\frac{\text{d}^2}{\text{d}t^2} z_s = -2N\xi^2 \frac{N+1}{N} (z_s - z_\infty) - \alpha \frac{\text{d}z_s}{\text{d}t}. \tag{24}$$

Another scenario where a closed solution can be obtained is weak system-bath coupling. In the weak coupling limit $z_1 = z_2 = ... = z_N \neq z_s$. As before the average polarization is a conserved quantity so we can write $z_k(t) = [(N+1)z_\infty - z_s(t)]/N$ and get

$$\frac{\mathrm{d}^2}{\mathrm{d}t^2}z_s = -2(\sum_{k=1}^{N}\xi_{sk}^2)\frac{N+1}{N}(z_s - z_\infty) - \alpha\frac{\mathrm{d}z_s}{\mathrm{d}t}, \tag{25}$$

which has the same form as (24) just with different coupling strength.

Appendix C. External dephasing as a free resource

In our model, the decoherence is generated by another external environment (not the N-spin microbath). Yet, we consider it as a free resource for the following reasons. First, unlike thermalization, dephasing is often very easy to engineer or to add to existing schemes (see the ion trap and superconducting circuit realization proposals in this paper). Second, dephasing does not change the energy distribution so it cannot generate work or heat flows. That is, the dephasing environment is energetically useless. In our setup, the energy exchange with the system comes only from the microbath (spins 1 to N). Third, the dephasing environment can only increase the entropy of the elements it interacts with—it cannot be used as a resource for entropy reduction. This is different from the coherence fuel used in [48] which should be treated as a valuable consumed resource.

Appendix D. An extended dephasing time in dephased microbaths $T_2 \leq 2\frac{N+1}{N}T_1$

Consider a completely positive Markovian map (11) with $H = 0$ for simplicity. z_0 is the asymptotic polarization of the map. The polarization of the system $\langle\sigma^z\rangle$ can be changed by setting the Lindblad operators to $A_1 = \sqrt{g_+}\sigma^+$, $A_2 = \sqrt{g_-}\sigma^-$. We start by studying a map with time-independent asymptotic polarization $\frac{\mathrm{d}z_0}{\mathrm{d}t} = 0$ and get from (11)

$$\frac{\mathrm{d}}{\mathrm{d}t}z = -2(g_+ + g_-)(z - z_0), \tag{26}$$

$$z_0 = \frac{1}{2}\frac{g_+ - g_-}{g_+ + g_-}. \tag{27}$$

The coherence dynamics is obtained by looking on $\langle x\rangle = \mathrm{tr}[\rho\sigma^x]$ that satisfies

$$\frac{\mathrm{d}}{\mathrm{d}t}x = -(g_+ + g_-)x. \tag{28}$$

The solutions of (26) and (28) are

$$\frac{z(t) - z_0}{z(0) - z_0} = \exp[-2(g_+ + g_-)t] \triangleq \mathrm{e}^{-\gamma_z t}, \tag{29}$$

$$\frac{x(t)}{x(0)} = \exp[-(g_+ + g_-)t] \triangleq \mathrm{e}^{-\gamma_x t}. \tag{30}$$

Using these solution we compare the polarization decay rate γ_z and the coherence decay rate γ_x and get

$$\frac{\gamma_z}{\gamma_x} = 2. \tag{31}$$

Adding elements like $A_3 = \sigma_z$ will increase $\frac{\mathrm{d}}{\mathrm{d}t}x$ but will not affect $\frac{\mathrm{d}}{\mathrm{d}t}z$ and therefore we get the standard result for completely positive Markovian dynamics [35, 36]

$$\gamma_z \leqslant 2\gamma_x. \tag{32}$$

Most importantly, we have used the fact that $\frac{\mathrm{d}z_0}{\mathrm{d}t} = 0$. In our case the map is *time-dependent*. The rate $(g_+ + g_-)$ is fixed by the physical couplings, but z_0 (related to $g_+ - g_-$) changes in time since the bath is finite. Using the polarization conservation $z_0(t) = \frac{(N+1)z_\infty - z_s}{N}$ we find

$$\frac{\mathrm{d}}{\mathrm{d}t}z_s = -2(g_+ + g_-)\frac{N+1}{N}(z_s - z_\infty), \tag{33}$$

and therefore

$$\gamma_z \leqslant 2\frac{N+1}{N}\gamma_x. \tag{34}$$

Thus, the polarization decay rate can be faster than the minimal value of $2\gamma_x$ allowed for Markovian maps with a *time-independent* z_0 (or alternatively the dephasing time is longer). Note that this dressing effect does not happen for x since the dephasing constantly eliminates any bath coherence that may arise from interacting with the system.

Appendix E. Experimental realization in ion traps

To synthesize significant pseudo-spin interaction Hamiltonians between the ions in the trap, spin-dependent forces are used. These forces can be realized, for example, by optical fields acting on optically separated pseudo-spin levels, or by Raman transitions on microwave-separated pseudo-spin levels. Spin-dependent forces induce spin-dependent motion of ions in the trap, leading to the acquisition of spin-dependent phases, and thus to an effective spin–spin interaction. To mimic the effect of spin interaction Hamiltonians and not only their time-evolution operator at specific times, quantum simulations are conducted using spin-dependent forces that are tuned far off-resonance from one, or more, of the crystal normal modes of motion. Thus, excited motion can be adiabatically eliminated and the interaction between the spins becomes direct. Here, spin–spin interaction can be thought of as mediated by the exchange of virtual crystal-phonons. A transverse field in the z direction can be introduced by detuning the pseudo-spin transition from the Raman or optical interaction. The dephasing of microbath spins is straightforward to implement using individual-addressing of bath ions with off-resonant laser beams that will shift them from resonance in a quasi-random time sequence.

The implementation of different $\xi_{i,j}$, depends on the normal modes of motion that are used. This can be done by spectrally tuning the lasers or microwave fields that induce spin-dependent forces. ATA coupling can be achieved in ion traps by tuning spin-dependent forces close to the center-of-mass mode of an ion crystal in which all ions oscillate in-phase, and with equal amplitude along the trap axis [42]. Thus the ATA configuration can be readily implemented. The use of spin-dependent forces that act on radial normal modes in ions traps was shown to lead to relative flexibility in determining $\xi_{i,j}$. In particular it was shown that when radial modes are spectrally closely-spaced, the range of spin–spin interactions can be scanned between $0 \leqslant \delta \leqslant 3$ where $\xi_{i,j} \propto 1/|i-j|^{\delta}$ and i and j are the locations of the ions in the chain, by tuning the spin-dependent force frequency close to or far from the radial modes respectively [49]. While the synthesis of arbitrary $\xi_{i,j}$ was shown to be possible [50] it will be very difficult to experimentally implement. The implementation of the NN configuration will, therefore, be challenging using trapped-ion systems, although it could be fairly well approximated using $\xi_{i,j} \propto 1/|i-j|^3$ where the next-to-nearest neighbor interaction is suppressed by a factor of eight.

Appendix F. Experimental realization in superconducting circuits

For definiteness, we focus on superconducting qubits of the transmon-type [45]. These qubits have good coherence properties, can be individually addressed, made to interact, and read out with high fidelity. Hence, they are currently being considered as building blocks for quantum computation [51]. In particular, they were recently used to study thermalization of an isolated quantum system [52]. The interaction between any pair (i,j) of qubits can be realized using a common resonator as quantum bus [53, 54] and takes the form $H_I = g_i g_j(\Delta_i^{-1} + \Delta_j^{-1})(\sigma_{+,j}\sigma_{-,i} + \sigma_{+,i}\sigma_{-,j})$, where g_i are the qubit-resonator couplings, $\Delta_i = \omega_i - \omega_r$ is the detuning between the qubit frequency ω_i and the resonator frequency ω_r, and the expression is valid in the strong-detuning limit, $\Delta_i/g_i \gg 1$. This interaction realizes a two-qubit $\sqrt{\text{iSWAP}}$ gate, mediated by virtual interaction with the resonator. The interaction is effectively switched off by 'parking' the qubits in a largely detuned configuration, and switched on by non adiabatically tuning the qubits in resonance with each other and closer in frequency to the resonator (the qubit frequencies can be adjusted on a fast time scale by changing the local magnetic field at each qubit's site). The NN scheme can be realized by arranging the qubits in a one-dimensional chain and coupling each neighboring pair by an individual bus resonator [55]. The ATA scheme can be realized by coupling all qubits to a common resonator, as recently demonstrated for an ensemble of ten qubits in [56]. Based on these experiments, we estimate that a tunable interaction strength $\xi/2\pi = 5$ MHz can be reached in both configurations. Single-qubit dephasing of arbitrary strength can be engineered by injecting classical noise into the system, causing fluctuations in the local magnetic field and hence in the qubit frequency. Due to spurious coupling to uncontrolled degrees of freedom, the superconducting qubits have an intrinsic thermalization time T_1. We require that the thermalization rate of the system via the dephased bath be much larger than its intrinsic relaxation rate, $\xi^2/\alpha \gg 1/T_1$, so that the composite system can be considered as isolated during the initial thermalization time. At the same time, observing the full crossover between unitary dynamics and Zeno freezing requires $\xi/\alpha \ll 1$. Even assuming a conservative $T_1 \approx 10\ \mu$s, ratios as low as $\xi/\alpha \approx 1/20$ can be attained with intrinsic relaxation still playing a negligible role.

References

[1] Seifert U 2012 *Rep. Prog. Phys.* **75** 126001
[2] Harris R and Schütz G 2007 *J. Stat. Mech.* P07020
[3] Goold J, Huber M, Riera A, del Rio L and Skrzypczyk P 2016 *J. Phys. A: Math. Theor.* **49** 143001
[4] Vinjanampathy S and Anders J 2016 *Contemp. Phys.* **57** 545–79
[5] Millen J and Xuereb A 2016 *New J. Phys.* **18** 011002
[6] Gour G, Müller M P, Narasimhachar V, Spekkens R W and Halpern N Y 2015 *Phys. Rep.* **583** 1–58
[7] Lostaglio M, Jennings D and Rudolph T 2015 *Nat. Commun.* **6** 6383
[8] Uzdin R 2017 *Phys. Rev.* E **96** 032128
[9] Mitchison M T, Woods M P, Prior J and Huber M 2015 *New J. Phys.* **17** 115013
[10] Uzdin R, Levy A and Kosloff R 2015 *Phys. Rev.* X **5** 031044
[11] Uzdin R 2016 *Phys. Rev. Appl.* **6** 024004
[12] Niedenzu W, Gelbwaser-Klimovsky D, Kofman A G and Kurizki G 2016 *New J. Phys.* **18** 083012
[13] Breuer H-P and Petruccione F 2002 *Open Quantum Systems* (Oxford: Oxford University Press)
[14] Ziman M, Štelmachovič P and Bužek V 2005 *Open Syst. Inf. Dyn.* **12** 81
[15] Diósi L, Feldmann T and Kosloff Ronnie R 2006 *Int. J. Quantum Inf.* **04** 99–104
[16] Gennaro G, Benenti G and Palma G M 2008 *Europhys. Lett.* **82** 20006
[17] Gennaro G, Benenti G and Palma G M 2009 *Phys. Rev.* A **79** 022105
[18] Rybár T, Filippov S N, Ziman M and Bužek V 2012 *J. Phys. B: At. Mol. Opt. Phys.* **45** 154006
[19] Bodor A, Diósi L, Kallus Z and Konrad T 2013 *Phys. Rev.* A **87** 052113
[20] Uzdin R and Kosloff R 2014 *New J. Phys.* **16** 095003
[21] Strasberg P, Schaller G, Brandes T and Esposito M 2017 *Phys. Rev.* X **7** 021003
[22] Scovil H E D and Schulz-DuBois E O 1959 *Phys. Rev. Lett.* **2** 262–3
[23] Geva E and Kosloff R 1994 *Phys. Rev.* E **49** 3903–18
[24] McMahon P L *et al* 2016 *Science* **354** 614–7
[25] Schlosshauer M A 2007 *Decoherence: and the Quantum-to-Classical Transition* (Berlin: Springer Science & Business Media)
[26] Kofman A G and Kurizki G 2000 *Nature* **405** 546
[27] Erez N, Gordon G, Nest M and Kurizki G 2008 *Nature* **452** 724
[28] Auffèves A, Gerace D, Gérard J M, Santos M F, Andreani L and Poizat J P 2010 *Phys. Rev.* B **81** 245419
[29] Rao D B and Kurizki G 2011 *Phys. Rev.* A **83** 032105
[30] Chenu A, Beau M, Cao J and Del Campo A 2017 *Phys. Rev. Lett.* **118** 140403
[31] De Raedt H, Jin F, Katsnelson M I and Michielsen K 2017 *Phys. Rev.* E **96** 053306
[32] Verstraete F, Wolf M M and Cirac J I 2009 *Nat. Phys.* **5** 633
[33] Brask J B, Haack G, Brunner N and Huber M 2015 *New J. Phys.* **17** 113029
[34] Tacchino F, Auffèves A, Santos M and Gerace D 2018 *Phys. Rev. Lett.* **120** 063604
[35] Gorini V and Kossakowski A 1976 *J. Math. Phys.* **17** 1298
[36] Chang T M and Skinner J 1993 *Physica* A **193** 483–539
[37] Suárez A, Silbey R and Oppenheim I 1992 *J. Chem. Phys.* **97** 5101–7
[38] Seifert U 2016 *Phys. Rev. Lett.* **116** 020601
[39] Jarzynski C 2017 *Phys. Rev.* X **7** 011008
[40] Miller H J D and Anders J 2017 *Phys. Rev.* E **95** 062123
[41] Strasberg P and Esposito M 2017 *Phys. Rev.* E **95** 062101
[42] Friedenauer A, Schmitz H, Glueckert J T, Porras D and Schätz T 2008 *Nat. Phys.* **4** 757–61
[43] Kim K, Chang M S, Korenblit S, Islam R, Edwards E, Freericks J, Lin G D, Duan L M and Monroe C 2010 *Nature* **465** 590–3
[44] Jurcevic P, Lanyon B P, Hauke P, Hempel C, Zoller P, Blatt R and Roos C F 2014 *Nature* **511** 202–5
[45] Koch J, Yu T M, Gambetta J, Houck A A, Schuster D I, Majer J, Blais A, Devoret M H, Girvin S M and Schoelkopf R J 2007 *Phys. Rev.* A **76** 042319
[46] Gasparinetti S, Solinas P, Pugnetti S, Fazio R and Pekola J P 2013 *Phys. Rev. Lett.* **110** 150403
[47] Reeb D and Wolf M M 2015 *IEEE Trans. Inf. Theory* **61** 1458–73
[48] Scully M O, Zubairy M S, Agarwal G S and Walther H 2003 *Science* **299** 862
[49] Kim K *et al* 2011 *New J. Phys.* **13** 105003
[50] Korenblit S *et al* 2012 *New J. Phys.* **14** 095024
[51] Devoret M and Schoelkopf R J 2013 *Science* **339** 1169–74
[52] Neill C *et al* 2016 *Nat. Phys.* **12** 1037
[53] Blais A, Huang R S, Wallraff A, Girvin S M and Schoelkopf R J 2004 *Phys. Rev.* A **69** 062320
[54] Blais A, Gambetta J, Wallraff A, Schuster D I, Girvin S M, Devoret M H and Schoelkopf R J 2007 *Phys. Rev.* A **75** 032329
[55] Salathé Y *et al* 2015 *Phys. Rev.* X **5** 021027
[56] Song C *et al* 2017 *Phys. Rev. Lett.* **119** 180511